

# Basic Electrochemical Behavior of Ti–7Cu Alloys for Medical Applications

L.C. TSAO\*

Department of Materials Engineering, National Pingtung University of Science & Technology  
1, Hseuhfu Road, Neipu, 91201 Pingtung, Taiwan

The aim of this study was to investigate the effects of two different treatments, as-cast setup and solution heat treatment, on the general electrochemical corrosion resistance of Ti–7Cu alloy samples immersed in a 0.9 wt% NaCl solution at 25°C. The microstructure was examined by scanning electron microscopy and X-ray diffractometry. Corrosion behavior was tested by potentiodynamic polarization curves. Finer  $\alpha'$  martensite and Ti<sub>2</sub>Cu intermetallic particles were provided by casting and heat treated processes, respectively. The results indicated that only corrosion potential is significantly more noble in the heat treated sample, but other characteristics are only slightly different.

PACS: 68.35.bd, 68.37.Hk, 65.40.gk, 81.40.Cd

## 1. Introduction

Titanium (Ti) and its alloys possess the advantages of high specific strength, good osseointegration, superior corrosion resistance, and biocompatibility. Thus, alloys such as commercially pure titanium (CP-Ti) and Ti6Al4V are used for dental implants and dentures. However, CP-Ti alloy is considered to be one of the more problematic, mainly because of its high melting temperature (1670°C) and high chemical activation energy at high temperature. The alloy Ti6Al4V is the one most commonly used because of its superior physical and mechanical properties in comparison to CP-Ti alloy [1]. However, the harmful elements V and Al present in Ti6Al4V tend to be released into the human body [2, 3]. Hence, additional alloying elements need to be added to make this alloy biocompatible and decrease its liquidus temperature.

One of these elements is copper, which not only decreases the melting point of the alloy [4] but also provides adequate biocompatibility [5] and reasonable corrosion resistance [6, 7]. Casting procedures are greatly favored. Kikuchi et al. reported that Ti–Cu alloys may present very high mechanical strength associated with good formability [6]. The Ti–Cu system presents an eutectoid transformation with 7.1%Cu (wt%) at 790°C; under these conditions,  $\alpha$ -Ti and Ti<sub>2</sub>Cu are formed [8].

Many studies have been also published on the corrosion behavior of CP-Ti alloy in artificial saliva, Ringer and Hanks' solutions, and others [9–11]. The high corrosion resistance of these alloys is due to the formation

on its surface of an adherent and highly protective oxide film, mainly formed of TiO<sub>2</sub> [12]. In addition, the microstructure of metallic alloys plays an important role in the mechanical properties and corrosion behavior of as-cast components [13–15].

The aim of this study was to evaluate the general electrochemical corrosion resistance of Ti7–Cu alloy samples obtained by casting and heat treatment. Potentiodynamic anodic polarization techniques was investigated in 0.9 wt% NaCl solution at 25°C.

## 2. Experimental procedure

Commercially pure metals (Ti 99.8 wt% and Cu 99.99 wt%) were used to prepare the Ti7–Cu alloy (wt%), which is a nearly eutectoid alloy, respectively, according to the Ti–Cu equilibrium phase diagram [8]. An as-cast Ti–7Cu sample was prepared by arc-melting its constituent using a current of 300 A on a water-cooled copper hearth under a pure Ar gas atmosphere. The as-cast Ti–7Cu alloy was repetitively melted and solidified with turning of the solidified ingots so as to obtain a completely alloyed state. Heat treated samples cut from the ingot were homogenized at 950°C for 2 h and then quenched in water. Hardness measurements, phase identification, and microstructure and corrosion analyses were then carried out on the as-cast and heat treated samples. Measurements were made at a minimum of five points on each specimen and averaged. X-ray diffraction (XRD, D/max 2500 V/PC) analysis was performed to determine the phase composition of the specimens. All specimens were ground with silicon carbide papers up to 2000 mesh, polished, and etched to reveal the microstructure (Keller's etchant, 1 mL of HF, 2.5 mL of HNO<sub>3</sub>,

\* e-mail: tlclung@mail.npust.edu.tw

1.5 mL of HCl and 95 mL of H<sub>2</sub>O). The microstructure of the alloys was examined by optical microscopy (OM) and scanning electron microscopy (SEM).

Potentiodynamic polarization were carried out in 0.9 wt% NaCl solutions. A saturated calomel reference electrode (SCE) and a platinum (Pt) counter-electrode were used. Prior to testing, the specimens were ground with 1200 grit SiC paper and cleaned in acetone for 2 min. These tests were conducted by stepping the potential, using a scan rate of 1 mV/s from  $-0.800/+2000$  mV (SCE).

### 3. Results and discussion

The micrographs of as-cast and heat treated Ti-7Cu alloy samples are shown in Figs. 1 and 2, respectively. The microstructure of a rapidly solidified Ti-7Cu alloy sample is depicted in the OM and SEM micrographs of Fig. 1. Figure 1a shows  $\alpha'$ -martensite plates of different sizes, which propagate within the pre-existing  $\beta$ -grains. Figure 1b shows the same microstructure in a high magnification back-scattered electrons (BSE) image. It is found that the martensite structure was combined with basket-weave structure of acicular  $\alpha$ -Ti (dark colour) and Ti<sub>2</sub>Cu (light colour). Williams et al. [16] reported that martensite has a massive morphology in alloys containing 4% Cu or less, whereas alloys containing 6 and 8% Cu exhibit acicular martensite. The high cooling rate imposed on the samples promoted complete  $\beta$ -phase decomposition and formed acicular plates of martensite typically found in titanium alloys. Souza et al. [17] found  $\alpha'$  martensite only with cooling rates higher than 9°C/s, as the volume fractions of eutectoid and martensite depend on the magnitude of the cooling rate. In addition, they found that Ti<sub>2</sub>Cu may occur as spherical precipitates when high cooling rates are applied. The same phenomenon was also observed in the present work. Cardoso et al. [18] reported that rapidly quenched near-eutectoid Ti-Cu alloys present Ti<sub>2</sub>Cu precipitates. Regardless of the cooling rate applied, such precipitation is unavoidable. The microstructure of the as-cast samples (in a copper mold) is in good agreement with the results from Cardoso et al.

Slow cooling of eutectoid Ti-7Cu alloy allowed eutectoid transformation to take place. An OM image of the slow cooled sample (Fig. 2a) shows an alternate typical basket-weave microstructure composed of lamellae of  $\alpha$ -Ti and Ti<sub>2</sub>Cu lamellae, as well as  $\alpha$  lamellae. The detail seen in Fig. 2b shows the structure under higher magnification, revealing much larger lamellar Ti<sub>2</sub>Cu phase (needles) than those found in the as-cast sample (Fig. 2b). The microstructure of the as-cast and heat treated samples (Fig. 1 and Fig. 2) suggests that faster cooling hinders the growth of the  $\alpha$  phase and Ti<sub>2</sub>Cu phase, which is supported by the fact that the thickness of the plates decreases with a decreasing distance from the source of cooling.

Figure 3 shows the XRD patterns of Ti-7Cu alloys obtained in as-cast and heat treated samples. It is well recognized that the microstructure of Ti-Cu binary alloys

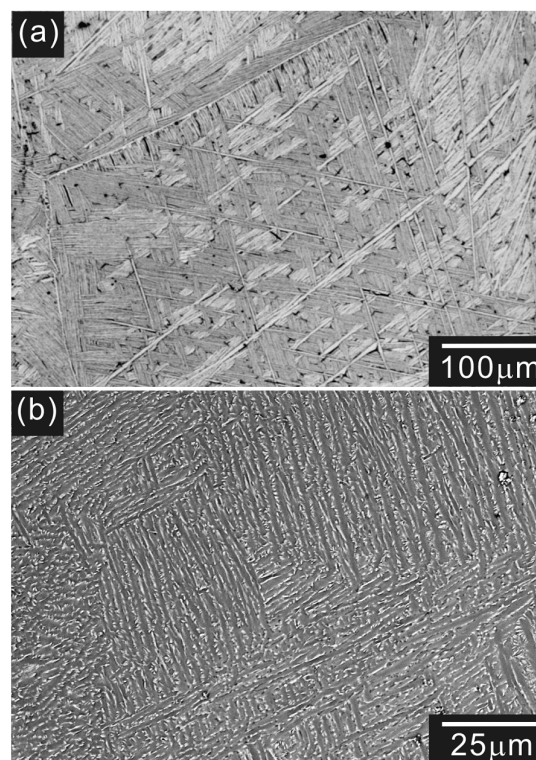


Fig. 1. Images of as-cast Ti-7Cu alloys: (a) OM, (b) SEM-BSE.

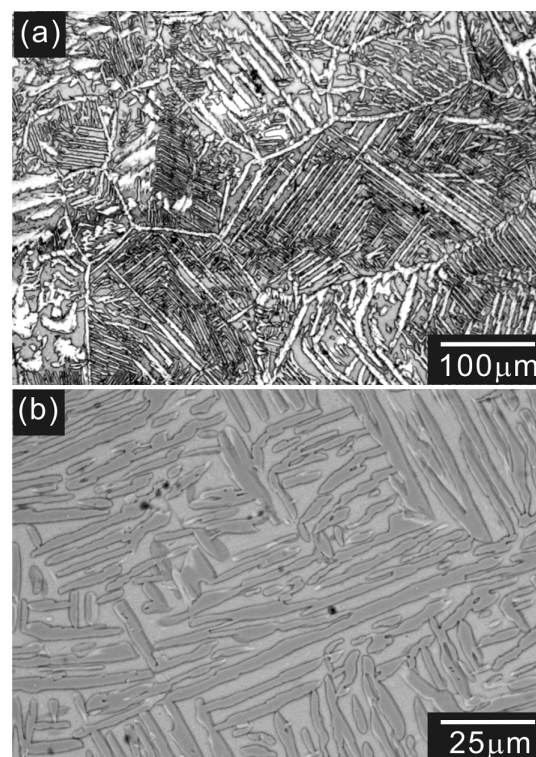


Fig. 2. Images of heat treated Ti-7Cu alloys: (a) OM, (b) SEM-BSE.

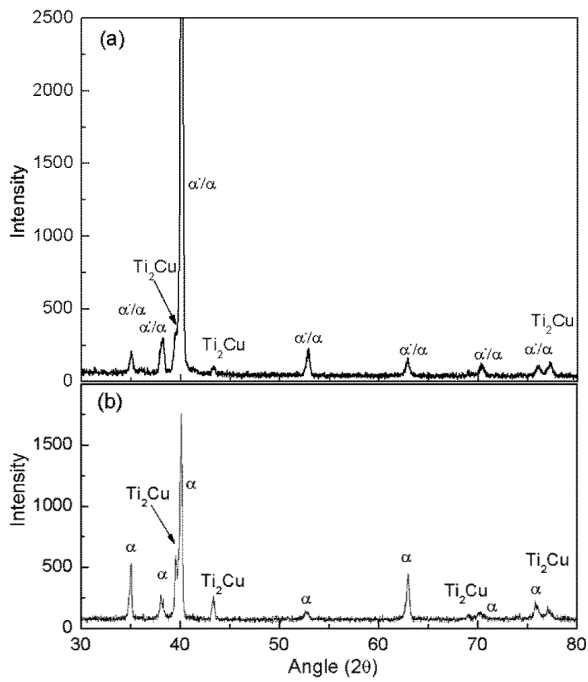


Fig. 3. X-ray diffraction patterns of: (a) as-cast sample and (b) heat treated sample.

with low Cu content contains  $\alpha$  phase and  $Ti_2Cu$  stable phases at room temperature [19]. The lattice parameters of  $\alpha$  phase in a Ti-Cu binary system were determined to have a hexagonal structure (space group  $P63/mmc$ ) with lattice parameters of  $a = 0.2945$  nm and  $c = 0.4685$  nm. Also, the crystallographic characteristics of  $Ti_2Cu$  compound are well defined in the literature as a tetragonal structure (space group  $I4/mmm$ ) with lattice parameters of  $a = 0.29438$  nm and  $c = 1.0786$  nm [20]. It was found that the X-ray diffraction patterns of as-cast samples showed both  $\alpha'$  martensite and  $\alpha$ -Ti phases and slight peaks associated with the intermetallic  $Ti_2Cu$ , as observed in Fig. 3a. However, the X-ray diffraction patterns of the  $\alpha$  phase and  $\alpha'$  martensite are remarkably similar which makes it difficult to differentiate the two phases. Additionally, the literature suggests that the lattice parameters of  $\alpha$  phase in titanium alloys changes as a function of the alloying element in solution with titanium. After heat treatment,  $\alpha$  peaks associated with  $Ti_2Cu$  were clearly detected, and the peak of  $\alpha'$  martensite disappeared, as shown in Fig. 3b. These XRD results are in agreement with the SEM observations.

Figure 4 shows the polarization curves of the as-cast samples and those after heat treatment in a 0.9 wt% NaCl solution. From the polarization curves, the corrosion potential ( $E_{corr}$ ), the primary passive current ( $I_{pp}$ ), the breakdown potential ( $E_b$ ), and the dynamic corrosion current density ( $I_{corr}$ ) were determined and are listed in Table. The dynamic corrosion current densities ( $I_{corr}$ ) were obtained from the polarization curves by the Tafel plots using both cathodic and anodic branches of the po-

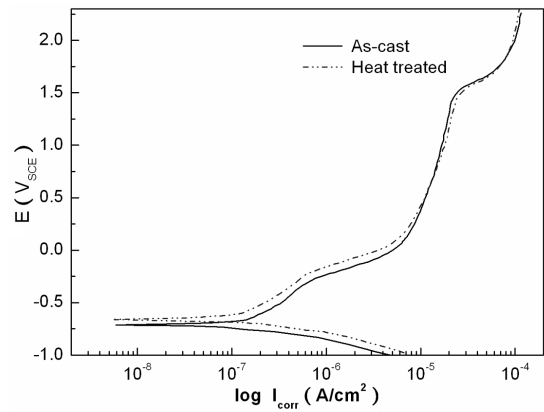


Fig. 4. Experimental potentiodynamic anodic polarization curves for Ti-7Cu alloys samples in a 0.9 wt% NaCl solution at 25 °C.

larization curves. The polarization curves have the same shape and are typical of passive behavior. The  $E_{corr}$  of the as-cast sample is  $-712 \pm 23$  mV<sub>SCE</sub>. Nevertheless, the  $E_{corr}$  of the Ti-7Cu alloy slightly shifted to positive values after heat treatment.

TABLE

Corrosion properties of the as-cast and heat treated Ti-7Cu alloys in a 0.9 wt% NaCl solution.

Specimens	$E_{corr}$ [mV <sub>SCE</sub> ]	$E_b$ [mV <sub>SCE</sub> ]	$\Delta E$ [mV]	$I_{corr}$ [nA/cm <sup>2</sup> ]	$I_{pp}$ [μA/cm <sup>2</sup> ]
as-cast	$-712 \pm 23$	$1516 \pm 50$	2228	$139 \pm 14$	$7.4 \pm 0.6$
heat treated	$-527 \pm 18$	$1511 \pm 43$	2038	$105 \pm 11$	$10.2 \pm 0.9$

$E_{corr}$  — corrosion potential (mV<sub>SCE</sub>),

$E_b$  — breakdown potential (mV<sub>SCE</sub>),

$\Delta E = E_{corr} - E_b$ ,

$I_{corr}$  — corrosion current density (nA/cm<sup>2</sup>),

$I_{pp}$  — primary passive current.

On the other hand, the breakdown potential ( $E_b$ ) of the as-cast samples became much more noble than that of heat treated samples, and the slightly large value of  $\Delta E$  ( $= E_b - E_{corr}$ ;  $E_{corr}$  = corrosion potential) for the as-cast samples reveals more stable passivation characteristics. This indicates that the pitting corrosion tendency of the as-cast sample can be alleviated due to elimination of the pitting nucleation sites in the matrix of the as-cast sample, in which a higher density of sub-micro  $Ti_2Cu$  phase and the  $\alpha'$  martensite of the microstructure exist in the as-cast sample. In addition, it can be seen that the  $I_{corr}$  of the as-cast specimen ( $139 \pm 10$  nA/cm<sup>2</sup>) is slightly higher than that of the alloy after heat treatment ( $105 \pm 11$  nA/cm<sup>2</sup>). These current densities, shown in Table, can be considered satisfactory when compared to the corresponding values obtained for CP-Ti and Ti6Al4V (of about 90 nA/cm<sup>2</sup>) [21] and quenched and heat treated Ti35Nb alloys (of about 60 nA/cm<sup>2</sup>) [22]. The different primary passive current densities ( $I_{pp}$ ) of as-cast ( $7.4 \pm 0.6$  μA/cm<sup>2</sup>) and heat treated Ti-Cu alloys ( $10.2 \pm 0.9$  μA/cm<sup>2</sup>) show similar

values. Recently, very similar  $I_{pp}$  measurements were also obtained for Ti–Nb–Zr as-cast alloys [23].

#### 4. Conclusions

From the present experimental investigation with as-cast and heat treated Ti–7Cu alloy samples, the following conclusions can be drawn:

1. The Ti<sub>2</sub>Cu phase is always present in the microstructure, regardless of the processing condition. In addition, after heat treatment, the volumetric fraction of Ti<sub>2</sub>Cu also increases.
2. The as-cast sample showed a finer  $\alpha'$  martensite structure combined with  $\alpha$ -Ti and Ti<sub>2</sub>Cu in the Ti–7Cu alloy when compared to the corresponding microstructures of the heat treated samples.
3. Both as-cast and heat treated samples present a passive behavior in this medium and high corrosion resistance. Nevertheless, their  $E_{corr}$  and the stability of their passive oxide films are quite similar.
4. The experimental results of corrosion tests have indicated that only corrosion potential is significantly more noble in the heat treated samples but other characteristics are only slightly different. For example, passive current density ( $I_{pp}$ ) is better in as cast alloy.

#### Acknowledgments

The authors acknowledge the financial support of this work from the National Science Council of Taiwan R.O.C. under project No. 101-2622-E-020-006-CC3.

#### References

- [1] L.C. Tsao, H.Y. Wu, J.C. Leong, C.J. Fang, *Mater. Des.* **34**, 179 (2012).
- [2] K.L. Wapner, *Clin. Orthop. Relat. Res.* **271**, 12 (1991).
- [3] H.J. Agins, N.W. Alcock, M. Bansal, E.A. Salvati, P.D. Wilson, P.M. Pellicci, P.G. Bullough, *J. Bone Joint Surg.* **70A**, 347 (1988).

- [4] C.M. Lee, C.P. Ju, J.H. Chern Lin, *J. Oral Rehabil.* **29**, 314 (2002).
- [5] C.F. Marcinak, F.A. Young, M. Spector, *J. Dent. Res.* **59**, 472 (1980).
- [6] M. Kikuchi, Y. Takada, S. Kiyosue, M. Yoda, M. Woldu, Z. Cai, O. Okuno, T. Okabe, *Dent. Mater.* **19**, 174 (2003).
- [7] M. Taira, J.B. Moser, E.H. Greener, *Dent. Mater.* **5**, 45 (1989).
- [8] J.L. Murray, *Phase Diagrams of Binary Titanium Alloys*, ASM International, Metals Park, Ohio, OH 1987.
- [9] J. Pan, D. Thierry, C. Leygraf, *Electrochim. Acta* **41**, 1143 (1996).
- [10] N. Ibris, J.C. Mirza-Rosca, *J. Electroanal. Chem.* **526**, 53 (2002).
- [11] A.K. Shukla, R. Balasubramaniam, S. Bhargava, *Intermetallics*. **13**, 631 (2005).
- [12] R.W. Schutz, *Handbook, Corrosion Materials*, ASM International, Materials Park (OH) 2005, p. 252.
- [13] W.R. Osorio, J.E. Spinelli, I.L. Ferreira, A. Garcia, *Electrochim. Acta* **52**, 3265 (2007).
- [14] W.R. Osorio, J.E. Spinelli, N. Cheung, A. Garcia, *Mater. Sci. Eng. A* **420**, 179 (2006).
- [15] D.Q. Martins, W.R. Osorio, M.E.P. Souza, R. Caram, A. Garcia, *Electrochim. Acta* **53**, 2809 (2008).
- [16] J.C. Williams, R. Taggart, D.H. Polonis, *Metall Trans B* **1**, 2265 (1970).
- [17] S.A. Souza, C.R.M. Afonso, P.L. Ferrandini, A.A. Coelho, R. Caram, *Mater. Sci. Eng. A* **29**, 1023 (2009).
- [18] F.F. Cardoso, A. Cremasco, R.J. Contieri, E.S.N. Lopes, C.R.M. Afonso, R. Caram, *Mater. Des.* **32**, 4608 (2011).
- [19] Z. Hu, Y. Zhan, J. She, G. Zhang, D. Peng, *J. Alloys Comp.* **485**, 261 (2009).
- [20] T.I. Bratanich, V.V. Skorokhod, O.V. Kucheryavyy, L.I. Kopylova, N.A. Krapivka, *Powder Metall. Met. Ceram.* **49**, 220 (2010).
- [21] Z. Cai, T. Shafer, I. Watanabe, M.E. Nunn, T. Okabe, *Biomaterials* **24**, 213 (2003).
- [22] A. Cremasco, W.R. Osorio, C.M.A. Freire, A. Garcia, R. Caram, *Electrochim. Acta* **53**, 4867 (2008).
- [23] D.Q. Martins, W.R. Osorio, M.E.P. Souza, R. Caram, A. Garcia, *Electrochim. Acta* **53**, 2809 (2008).